

Motivation

Conventional optoelectronic techniques have forced image sensors to a planar shape. Recent approaches relax this situation. For instance, silicon photodiodes are interconnected by elastomeric transfer elements for realizing a hemispherical detector geometry that mimics the shape of the human eye – theoretically enabling a wide field of view and low aberrations (Ko, et al., Nature 2008 [1]). Organic photodiodes, as another example, allow the application of inkjet digital lithography to implement sensors on fully flexible substrates (Ng, et. al., Applied Physics Letters 2008 [2]).

Thin-film luminescent concentrators (LCs) are polymer films doped with a fluorescent dye that absorbs light of a specific wavelength and re-emits it at a longer wavelength (cf. Figure 1). Waveguides based on an LC forward the emitted light towards the edges of the LC by total internal reflection at an attenuation that is proportional to the travel distance. They are normally used for increasing the efficiency of solar cells with respect to supporting larger incident angles. Photodiodes glued to the LC surface create an interface with higher optical density than air or the polymer of the LC. This causes light to be decoupled from the LC at the positions of the photodiodes. The attenuation of the measured light at these positions allows recovering the location of an incident light point via simple triangulation. Thus, LCs have also been used for camera-free laser-pointer tracking on large and scalable sensor surfaces (Koeppel, et al., Optics Express 2010 [3]).

LCs share several interesting properties: They are flexible, transparent, and low cost (and therefore scalable and disposable) polymer films. The state of the art that applies LCs for light sensing is currently only able to reconstruct simple point images. Our approach makes it possible to reconstruct entire images that are focused on the LC surface.

Compared to other methods, this is –to the best of our knowledge– the first attempt that enables a fully transparent (no integrated circuits or other structures), flexible (curved shapes), scalable (sensor size can be small to large at similar cost, pixel size is not restricted to size of the photodiodes), and disposable (the sensing area is low-cost and can be replaced if damaged) image sensor.

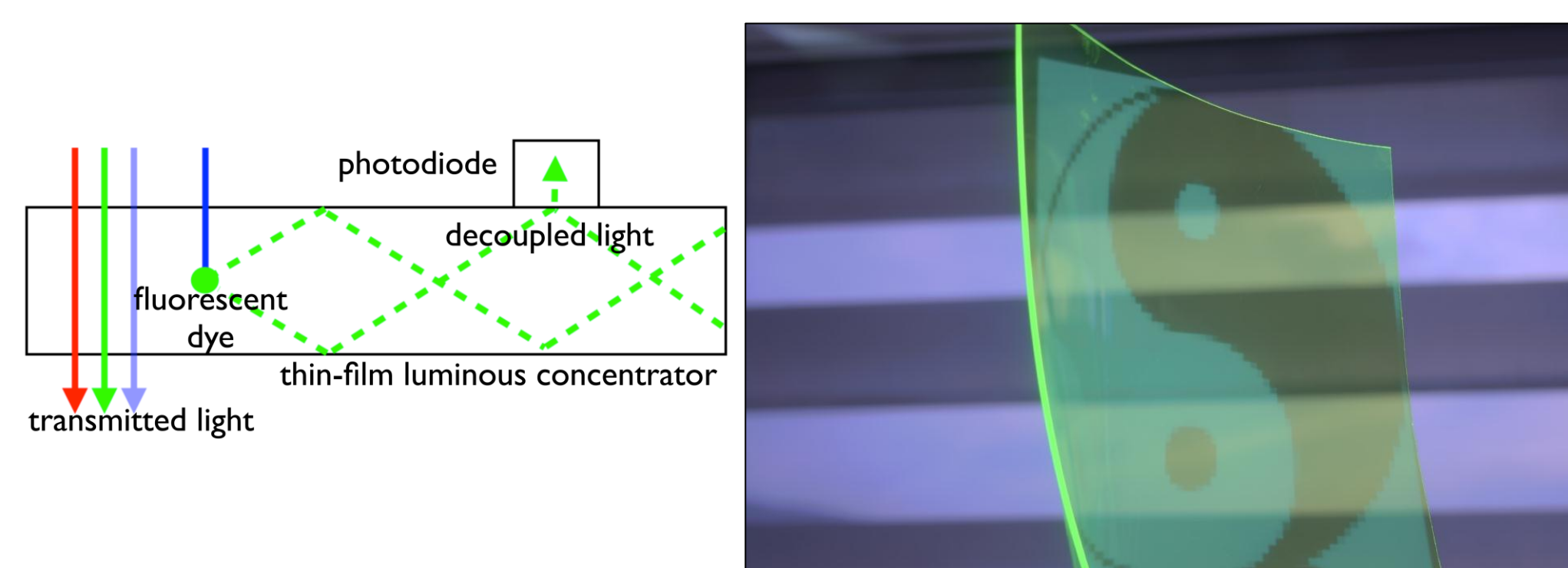


Figure 1: Thin-film luminescent concentrator (LC) principle (left) and example (right).

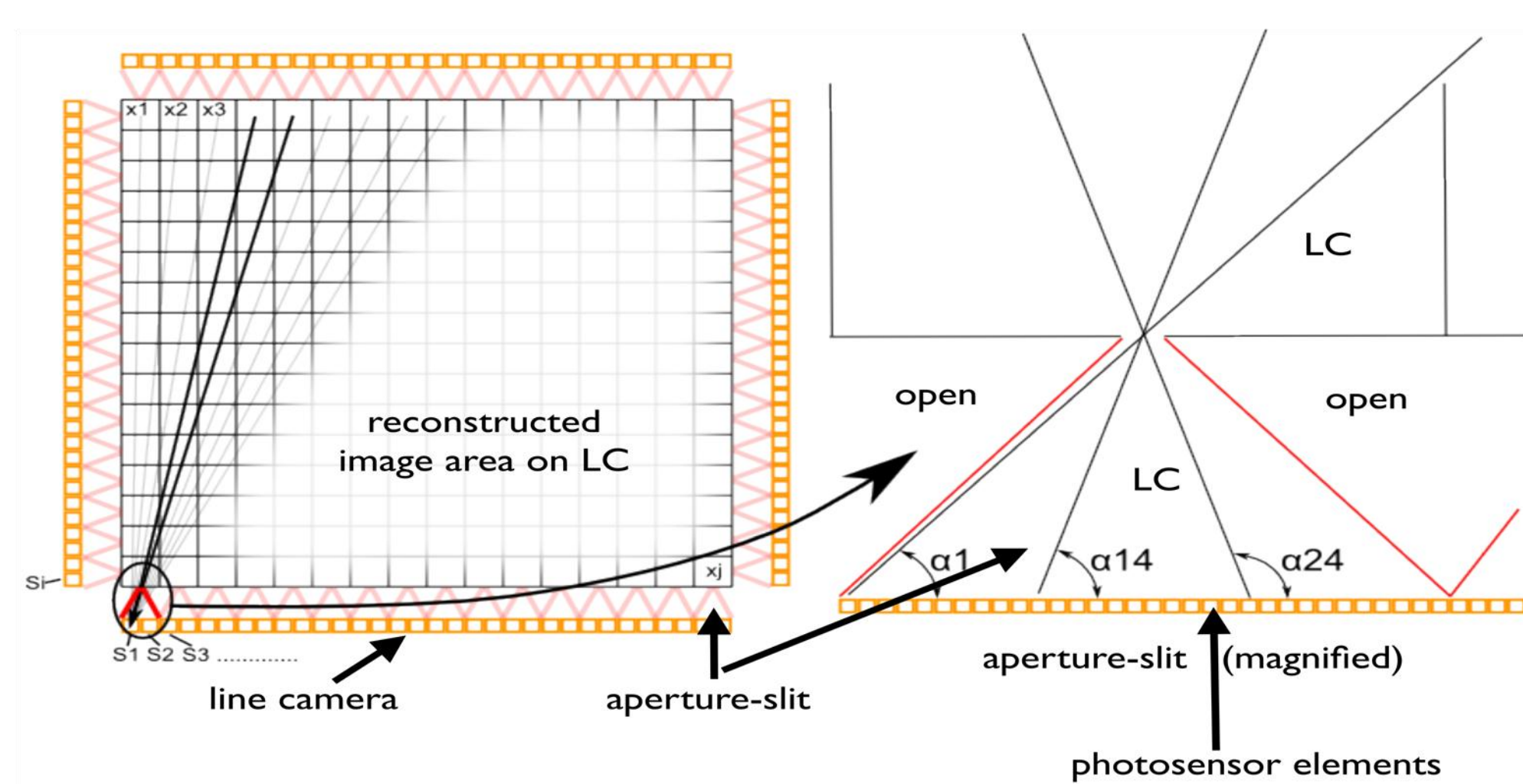


Figure 2: The film's edges are cut into triangular aperture slits and photodiodes (four line scan cameras) are placed on the surfaces of these slits. This measures the light transport of a two-dimensional light field within the LC film that can be used to reconstruct the image focused on the LC surface.

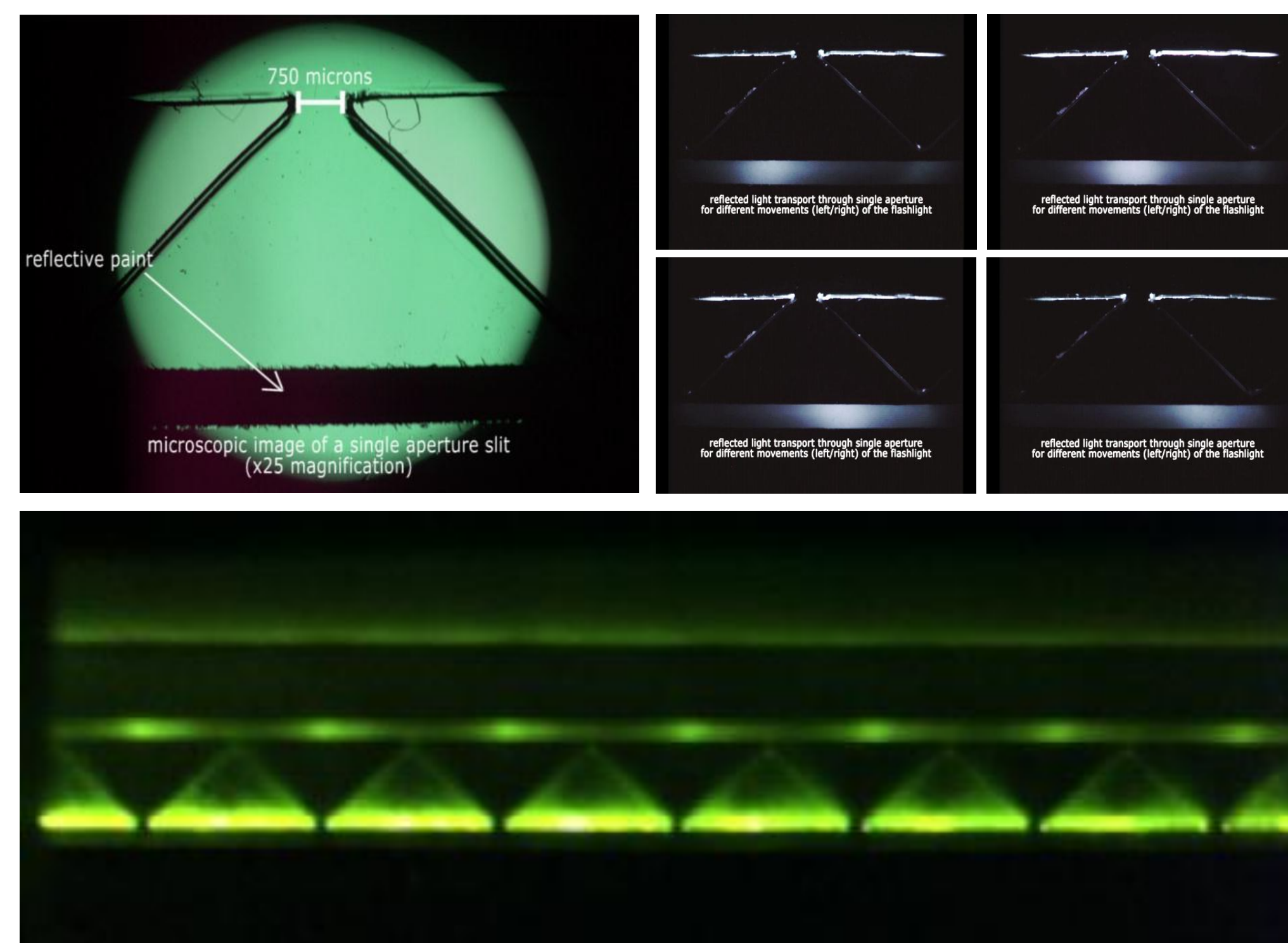


Figure 3: Microscopic view of slit aperture when decoupling the light signal from a moving flashlight (right to left on sensor area).

Image Reconstruction

The correlation of the transport losses between discrete entrance points (i.e., pixels p) on the LC surface with many photodiodes (s) placed at the boundary of the LC surface can be represented with $s = Tp$, where T is the light transport matrix that can be calibrated.

In principle, an image focused on the LC can be reconstructed with the inverse light transport ($p = T^{-1}s$), or with filtered backprojection. However, since each photodiode measures the integral of all pixel contributions, the light-transport matrix would be dense with a high condition number, and image reconstruction becomes very unstable (in particular in the presence of sensor noise). A tomographic reconstruction would be seriously undersampled.

For solving this problem, we cut the LC edges into triangular aperture slits and place the photodiodes appropriately on the surfaces of these slits (cf. Figures 2 and 3). Reflective paint at the backside of the slits causes a higher decoupling efficiency. With this, we are recording the transport of a two-dimensional light field within the LC film using multiple line scan cameras surrounding the imaging area. In this case, the light transport matrix becomes sparse, its condition number is reduced, and more positional and directional samples are available for a tomographic reconstruction. We apply SART for reconstruction (cf. Figure 4).

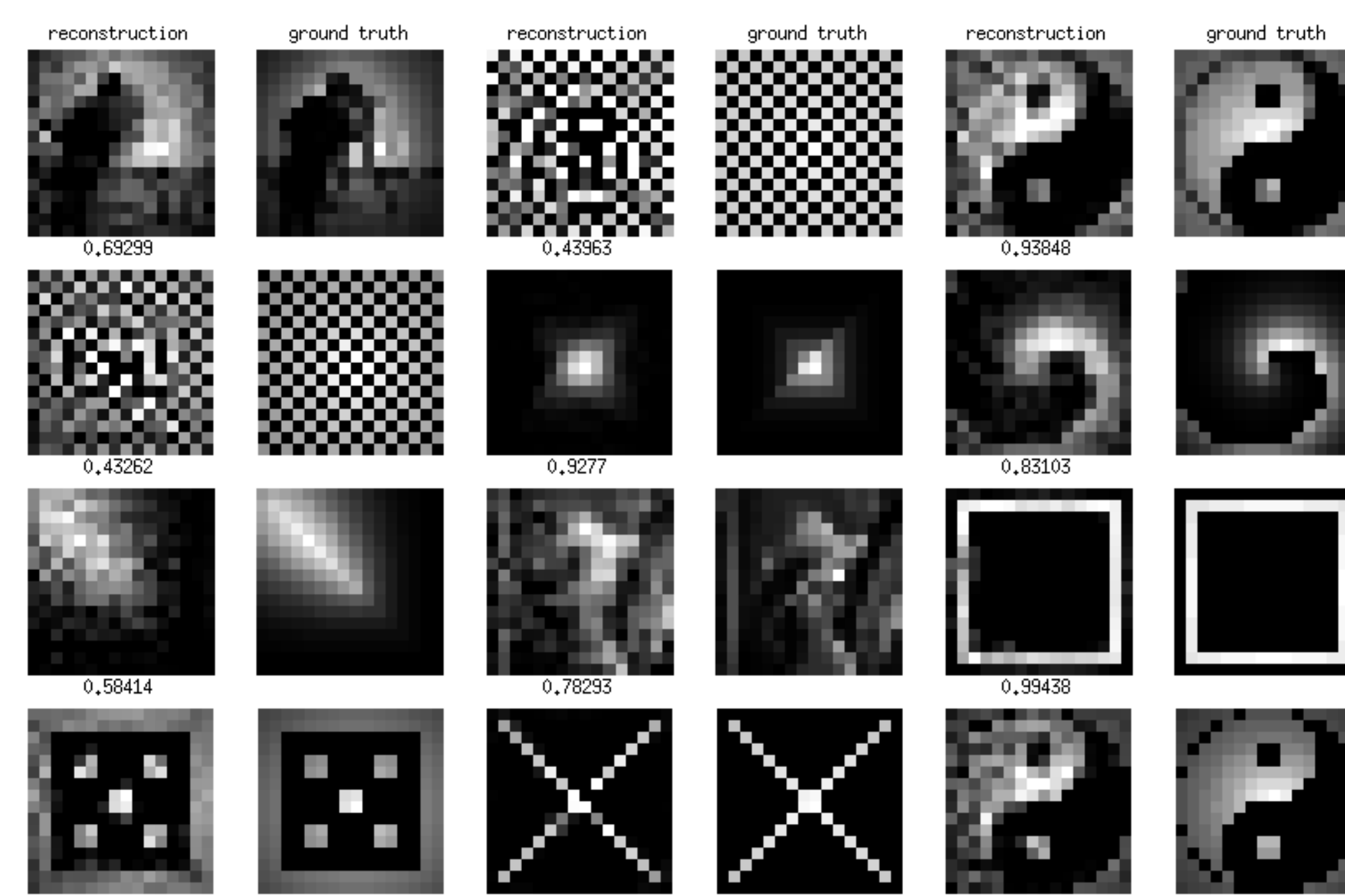


Figure 4: Reconstruction results for images with a resolution of 16x16 pixels, and comparison to ground truth (numbers indicate the structural similarity index SSIM [4]).

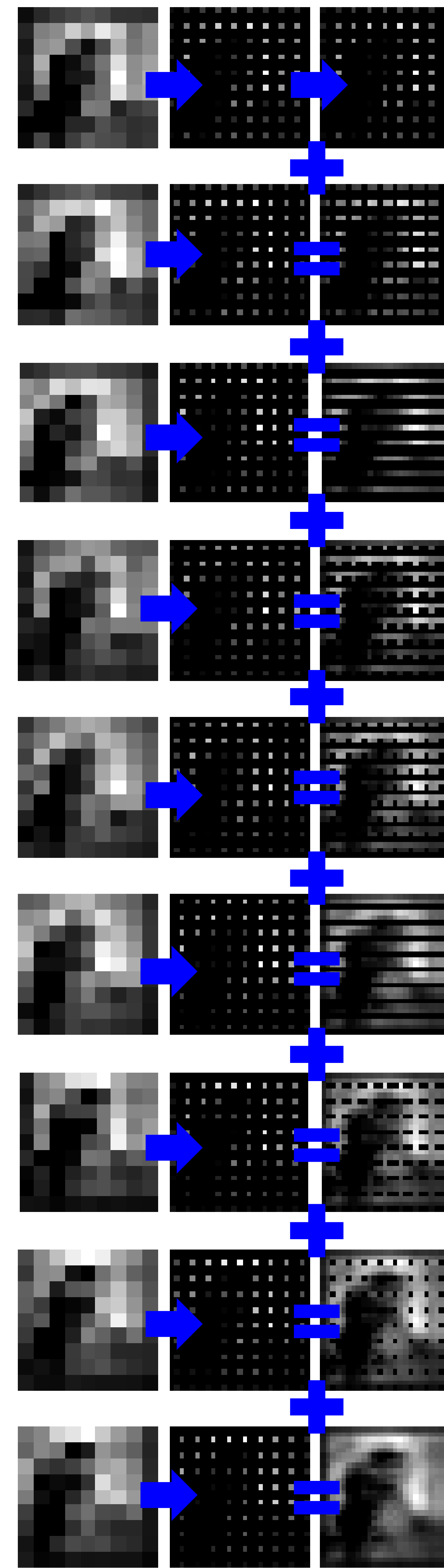


Figure 5: Step-by-step assembly of an image with a resolution of 27x27 pixels using 3x3 shifted reconstructions of images with a resolution of 9x9 pixels. The ground truth image and a direct reconstruction are shown on the right.

Super-Resolution

Solving large equation systems that are needed for the reconstruction of higher image resolutions is difficult and time consuming. Instead of reconstructing a high resolution image with a single high resolution transport matrix (resulting in a substantially large equation system), the same image can be approximated by combining the results of multiple low resolution reconstructions, that are created from shifted transport matrices.

Just as the image can be focused anywhere on the LC sensor area, the transport matrix can be calibrated at any position. The reconstructed pixels of an image contain the average of the light intensities that are focused onto the corresponding areas of the LC sensor area that are represented in the transport matrix.

For reconstructing a higher resolution image with lower resolution transport matrices, multiple matrices have to be calibrated at sub-pixel shifted positions on the LC sensor area. For example, if a transport matrix is used for reconstructing images with a resolution of 9x9 pixels, it has to be calibrated at 3x3 shifted (horizontally and vertically, by half-a-pixel distance) positions on the sensor area. This allows reconstructing nine images with a resolution of 9x9 pixels – each containing a slightly different intensity average within their pixels. These nine images can then be combined to a new image with a resolution of 27x27 pixel. Reconstructing and combining nine images with a resolution of 9x9 pixels is by a factor of 2 faster and much more stable than reconstructing an image of 27x27 pixels directly (cf. Figure 5). Figure 6 illustrates more examples.

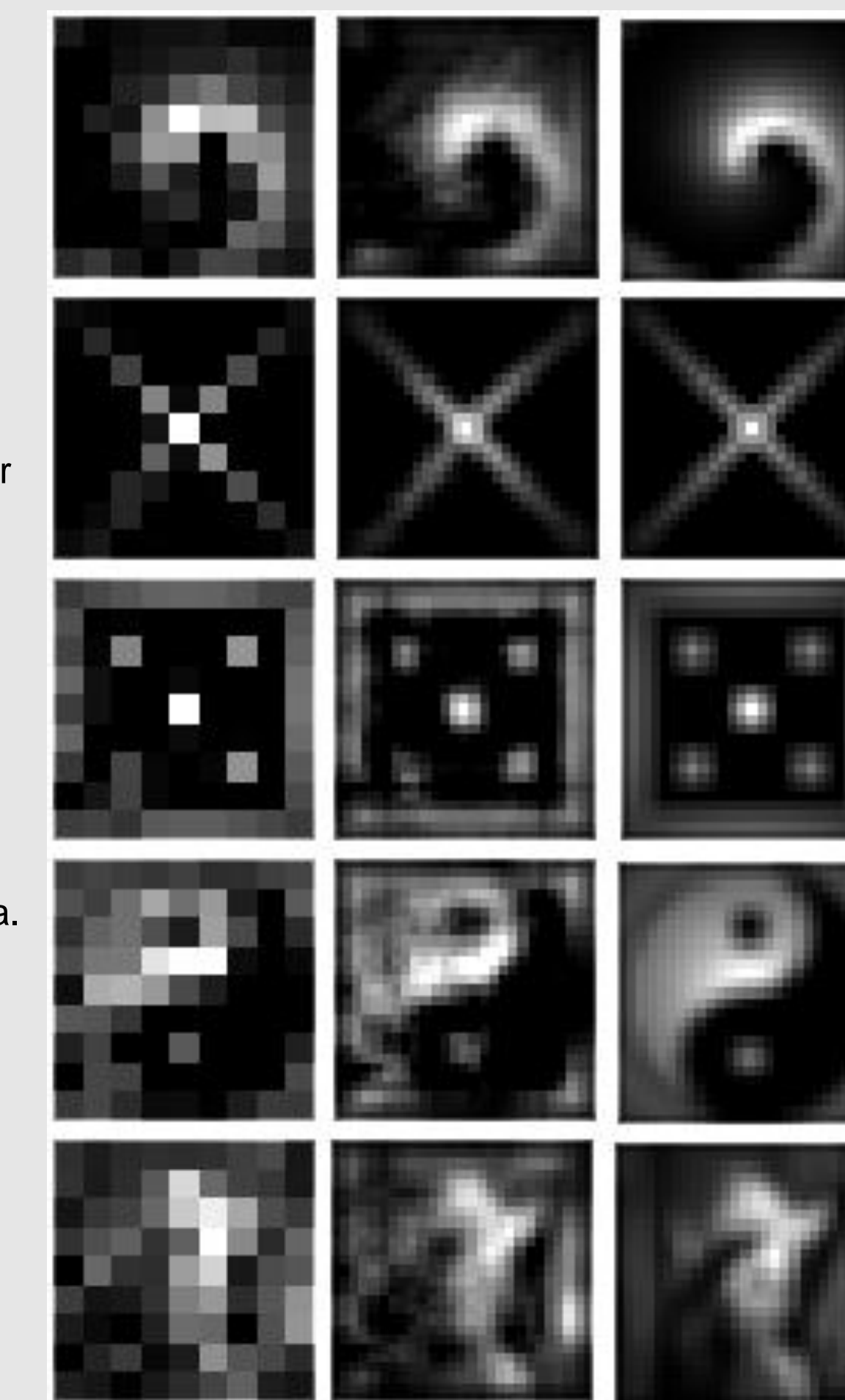


Figure 6: Further super-resolution examples (9x9 to 27x27). Note, that since the left line scan camera was damaged the left side of each reconstruction shows artifacts.

Future Work

We will investigate curved and flexible sensor shapes and the application of multiple stacked LC layers with different wavelength responses that enable the reconstruction of color images. We will also seek for more robust and faster image reconstruction techniques, and will explore new applications, such as novel non-touch interfaces.

References

1. H.C. Ko, M.P. Stoykovich, J. Song, V. Malyarchuk, W.M. Choi, C.J. Yu, J.B. Geddes Iii, J. Xiao, S. Wang, Y. Huang, et al. A hemispherical electronic eye camera based on compressible silicon optoelectronics. Nature, 454(7205):748–753, 2008.
2. T.N. Ng, W.S. Wong, M.L. Chabinc, S. Sambandan, and R.A. Street. Flexible image sensor array with bulk heterojunction organic photodiode. Applied Physics Letters, 92:213303, 2008.
3. R. Koeppel, A. Neuling, P. Bartu, and S. Bauer. Video-speed detection of the absolute position of a light point on a large-area photodetector based on luminescent waveguides. Optics Express, 18(3):2209–2218, 2010.
4. Z. Wang, A.C. Bovik, H.R. Sheikh, and E.P. Simoncelli. Image quality assessment: From error visibility to structural similarity. Image Processing, IEEE Transactions on, 13(4):600–612, 2004.

This project is supported by:

Microsoft
Research